Diagnostic challenges in primary cardiac lymphoma, the opportunity of ^{18}F-FDG PET/CT integrated with contrast-enhanced CT

Entao Liu,[a,b] Jia Huang,[c] Haojian Dong,[d] Zerui Chen,[e] Chao Liu,[f] Qiu Xie,[g] Weiping Xu,[b] Shuxia Wang,[b] and Zaiyi Liu[a,c]

[a] The Second School of Clinical Medicine, Southern Medical University, Guangzhou, China
[b] WeiLun PET Center, Department of Nuclear Medicine, Guangdong Provincial People's Hospital, Guangdong Academy of Medical Sciences, Guangzhou, China
[c] Department of Radiology, Guangdong Provincial People's Hospital, Guangdong Academy of Medical Sciences, Guangzhou, China
[d] Department of Cardiology, Vascular Center, Guangdong Provincial People's Hospital, Guangdong Academy of Medical Sciences, Guangzhou, China
[e] Department of Cardiovascular Surgery, Guangdong Provincial People's Hospital, Guangdong Academy of Medical Sciences, Guangzhou, China
[f] Department of Pathology and Laboratory Medicine, Guangdong Provincial People's Hospital, Guangdong Academy of Medical Sciences, Guangzhou, China
[g] Division of Adult Echocardiography, Guangdong Provincial People's Hospital, Guangdong Academy of Medical Sciences, Guangzhou, China

Received Feb 24, 2021; accepted Jun 22, 2021
doi:10.1007/s12350-021-02723-6

Background. **The purpose of this study was to retrospectively evaluate the value of ^{18}F-FDG PET/CT integrated with contrast-enhanced CT (CECT) in the differential diagnosis of primary cardiac lymphomas (PCLs) and primary cardiac angiosarcomas (PCAs).**

Methods. **Clinical and imaging data of patients with PCLs and PCAs were collected. All patients underwent preoperative ^{18}F-FDG PET/CT and thoracic CECT. The enhancement pattern and tumor morphology were analyzed using CECT images. The intensity- and volume-based PET parameters of cardiac lesions were analyzed. The performance characteristics of all parameters were assessed.**

Results. **Nine patients with PCL and eight patients with PCA were analyzed. There were significant differences in SUVmax (t = 3.790, P = .002), SUVmean (t = 4.273, P = .001), metabolic tumor volume (U = 13.00, P = .027), tumor-to-liver ratio (U = 10.00, P = .011), and total lesion glycolysis (U = 4.0, P = .001) between PCLs and PC^{18}As. There were significant differences in the enhancement pattern of tumors (P = .002) and tumor morphology (P = .015). The**

Supplementary Information The online version contains supplementary material available at (https://doi.org/10.1007/s12350-021-02723-6) contains supplementary material, which is available to authorized users.

Funding This research was funded by the Guangdong Medical Research Fund (No. A2020001), the Traditional Chinese Medicine Bureau of Guangdong Province (No. 20201003, No. 20211005), the National Science Fund for Distinguished Young Scholars (No. 81925023), and the National Natural Science Foundation of China (No. 81771912).

The authors of this article have provided a PowerPoint file, available for download at SpringerLink, which summarises the contents of the paper and is free for re-use at meetings and presentations. Search for the article DOI on SpringerLink.com.

Reprint requests: Zaiyi Liu, Department of Radiology, Guangdong Provincial People's Hospital, Guangdong Academy of Medical Sciences, Room 201, 2/F, WeiLun Building of Guangdong Provincial People's Hospital, 106 Zhongshan ER Road, Guangzhou510080, China; *zyliu@163.com*

1071-3581/$34.00

combination of F-FDG PET/CT and CECT improved the diagnostic accuracy, and the combination cutoff (SUVmean > 5.17) could reach 100%, but the difference was not statistically significant ($P > .05$).

Conclusion. **The intensity- and volume-based PET parameters of PCL were significantly higher than those of PCA. The enhancement pattern and tumor morphology were also different. According to these characteristics, the two most common types of primary cardiac malignancies can be differentiated. (J Nucl Cardiol 2022;29:2378–89.)**

Key Words: PET/CT • Tomography • X-ray computed • Cardiac tumors • Lymphoma • Angiosarcoma

Abbreviations

AUC	Area under the ROC curve
CECT	Contrast-enhanced CT
^{18}F-FDG	^{18}F-Fluorodeoxyglucose
LV	Left ventricular
LVR	Left ventricular ratio
MIP	Maximum intensity projection
MTV	Metabolic tumor volume
PCAs	Primary cardiac angiosarcomas
PCLs	Primary cardiac lymphomas
PET/MRI	Positron emission tomography/magnetic resonance imaging
PET/CT	Positron emission tomography/computed tomography
ROC	Receiver operating characteristic curve
SUVmax	Maximum standardized uptake value
SUVmean	Mean standardized uptake value
TLG	Total lesion glycolysis
TLR	Tumor-to-liver ratio
TTE	Transthoracic echocardiography

See related editorial, pp. 2390–2392

INTRODUCTION

Cardiac lymphoma is usually secondary to cardiac involvement by systemic lymphoma, and less than 25% of lymphomas have cardiac involvement.[1,2] In contrast, primary cardiac lymphomas (PCLs) are extremely rare, accounting for only 2% of primary cardiac tumors.[3–6] As of July 2018, only 232 cases of PCLs have been reported in the literature.[7] PCLs are highly invasive lymphomas, and the predominant histopathological type is diffuse large B-cell lymphoma, which accounts for 80% of published cases.[8,9] The average age of onset is 63 years, and the male-to-female ratio is 3:1.[4] The prognosis of this disease is poor, and the median survival time after diagnosis is 7 months.[8,10] Early diagnosis in conjunction with effective chemotherapy can relieve the pathogenetic condition, control the progress of the disease effectively, and result in good outcomes with long-term survival.[3,11,12] PCLs most frequently arise on the right side of the heart, particularly in the right atrium. This requires differentiation from cardiac angiosarcoma, which is the most common primary cardiac malignancy, often occurring on the right side of the heart.[13] There is a lack of comparative studies on different primary cardiac malignant tumors, especially PCLs and primary cardiac angiosarcomas (PCAs). Previous literature reports a considerable overlap of imaging characteristics between cardiac lymphomas and angiosarcomas, which brings great challenges to the diagnosis of PCLs based on morphologic features.[14] PET/CT or PET/MRI with contrast-enhanced imaging provides a combination of morphological tumor characterization and visualization of tumor metabolism. It has proven to be an indispensable problem-solving tool and is preferred for evaluation in lymphomas. Therefore, we retrospectively compared ^{18}F-FDG PET/CT with CECT images of patients with PCLs and PCAs to provide diagnostic and differential diagnoses.

METHODS

Study Design and Population

The local Institutional Review Board approved this retrospective study and waived the requirement for informed consent. We retrospectively collected clinical and imaging data of 139 consecutive patients with cardiac masses suspected by transthoracic echocardiography (TTE) and/or thoracic CT. All patients preoperatively underwent ^{18}F-FDG PET/CT, followed by thoracic CECT on the same day. All patients only received symptomatic treatment before the above examination. The final diagnosis was confirmed by histopathology.

Inclusion Criteria

Patients were included if they met all the following inclusion criteria: (i) the patients had no previous history of lymphoma; (ii) the patients only received symptomatic treatment and had no history of chemotherapy, radiotherapy, or surgical resection before the PET/CT scan; (iii) cardiac masses were confined to the heart or pericardium without extra-cardiac involvement on ^{18}F-

FDG PET/CT imaging; and (iv) the diagnosis was confirmed by histopathology.

Exclusion Criteria

Patients were excluded for any of the following: (i) incomplete image data sets, (ii) lack of the final histological diagnosis, (iii) if extra-cardiac lesions were found on ^{18}F-FDG PET/CT imaging or ^{18}F-FDG uptake of bone marrow or subcutaneous fascia was increased diffusely, and (iv) bone marrow infiltration was confirmed by histopathology.

Patient Preparation and PET/CT Protocol

All patients with suspected cardiac tumors received special diet preparation (high-fat, low-carbohydrate, and protein-permitted diet) and fasting for more than 12 hours before ^{18}F-FDG PET/CT examination. A detailed description of the preparation and the PET/CT protocol was provided in our previous study. [15]

Imaging Analysis

All images were transferred to the workstation (Syngo MI Workplace, version VA30A, Siemens Healthcare) and reviewed in standard planes. CECT images were reviewed by a radiologist (Dr. JH) who received standard training in cardiac imaging. PET/CT images were evaluated by an experienced nuclear physician (Dr. WX). An observer (Dr. SW) with more than ten years of experience in radiology and PET/CT diagnosis combined the above two imaging modalities to make the final assessment.

FDG PET/CT For the quantitative evaluation of the suppression of myocardial ^{18}F-FDG uptake by the special diet preparation, we used the left ventricular ratio (LVR) of left ventricular (LV) myocardial uptake to the LV blood pool uptake. To reduce observer dependence and improve reproducibility, we used the maximum standardized uptake value (SUVmax). We chose to measure the ventricular septum as myocardial intake to avoid interference caused by lymphoma involving the LV free wall. The SUVmax of the blood pool was measured in the LV area between the right inferior pulmonary vein and the coronary sinus. Considering that the interventricular septum thickness was not greater than 1.3 cm, we chose a region of interest (ROI) with a diameter of 1.5 ± 0.1 cm to measure the SUVmax of the ventricular septum and the left ventricular blood pool. According to the CECT image, the non-contrast CT image and PET image were matched to the same position to display the interventricular septum and ventricular cavity. For PET images, the ROI obtained in the CT image of each patient was taken as a template, and it was extrapolated to the PET image and subsequently quantified (Supplementary Material 1 for measurement methods). LVR was calculated by dividing the LV wall's SUVmax by the LV blood pool SUVmax. The calculation formula used is as follows:

$$\mathrm{LVR} = \frac{\mathrm{SUVmax\ of\ LV\ wall}}{\mathrm{SUVmax\ of\ LV\ blood\ pool}}.$$

For quantitative evaluations, the intensity- and volume-based PET parameters of cardiac lesions were analyzed. Intensity-based parameters included SUVmax, SUVmean, and tumor-to-liver ratio (TLR). TLR was calculated by dividing the cardiac lesion SUVmax by the liver SUVmean. Volume-based parameters included metabolic tumor volume (MTV) and total lesion glycolysis (TLG). A threshold of 41% of the SUVmax was used to delineate the MTV and TLG.[16,17] For qualitative evaluations, the diagnostic criteria for PET/CT are that a tumor with diffuse metabolism is diagnosed as lymphoma, while a tumor with focal metabolism is diagnosed as angiosarcoma.

CECT The enhancement pattern and tumor morphology were analyzed using CECT images. The pattern was categorized as heterogeneous or homogeneous enhancement, represented by 0 and 1, respectively (0 = heterogeneous and 1 = homogeneous enhancement). The tumor morphology was categorized as focal and diffuse lesions, represented by 0 and 1, respectively (0 = focal and 1 = diffuse lesions).[18] The diagnostic criteria for CECT are as follows: if the tumor is a homogeneous enhancement, the diagnosis is lymphoma; if the tumor is a heterogeneous enhancement, the diagnosis is angiosarcoma; if the tumor is a diffuse lesion, the diagnosis is lymphoma; if the tumor is a focal lesion, the diagnosis is angiosarcoma. When there is a conflict between the diagnostic criteria of enhancement pattern and tumor morphology and considering the possibility of intrapericardial metastasis in angiosarcoma, we specify the enhancement pattern as the primary principle. We also evaluated the coronary vessel floating sign in the arterial phase, represented by 0 and 1, respectively, to indicate whether there was such a sign (0 = no and 1 = vessel floating sign). Pleural effusion and pericardial effusion were analyzed on CECT, and 0, 1, 2, and 3 were used to represent none, mild, moderate, and severe, respectively.

Statistical Analysis

Continuous variables were presented as mean ± standard deviation, and categorical variables were presented as frequencies and percentages. The One-Sample *t* test was used to compare the mean of LVR to

one (test value). The Mann-Whitney U test or Student's *t* test was used to compare two independent groups. Receiver operating characteristic (ROC) analysis was performed to determine the area under the ROC curve (AUC) for the intensity- and volume-based parameters. Statistical analyses were performed using SPSS software (v.26.0) and MedCalc software (v.19.0.7). A two-tailed probability value of $< .05$ was considered statistically significant.

Table 1. Characteristics of patients (N = 17)

	All	Primary cardiac angiosarcomas	Primary cardiac lymphomas	*t* or *U* or χ^2	*P* value
Number of patients	17	8	9		
Age (years)	48.8 (16.0-68.0)	40.3 (16.0-65.0)	56.4 (31.0-68.0)	2.49	.025
Gender, n (%)					1.000*
Male	14	7	7		
Female	3	1	2		
Blood glucose level (mmol/L)	5.68	5.15	6.14	1.76	.099
^{18}F-FDG-injected dose (MBq)	408.3	431.5	387.7	− 1.11	.286
Location (*number of patients*)					.002*
Right atrium	10	8	2		
More than two chambers	7	0	7		
Treatment and histopathology					
Complete resection	5	5	0		
Partial resection	3	1	2		
Biopsy only	7	2	5		
Cytological examinations†	2	0	2		
Tumor classification		Angiosarcomas	DLBCL‡		
Pleural effusion				0.400	.527§
None	3	2	1		
Mild	7	1	6		
Moderate	5	4	1		
Severe	2	1	1		
Pericardial effusion				0.878	.349§
None	2	2	0		
Mild	7	1	6		
Moderate	5	2	3		
Severe	3	3	0		

*Fisher's Exact Test was used.
†Cytological examinations of pleural and pericardial effusions.
‡DLBCL, Diffuse Large B-cell Lymphoma.
§Chi Square for Trend was used.

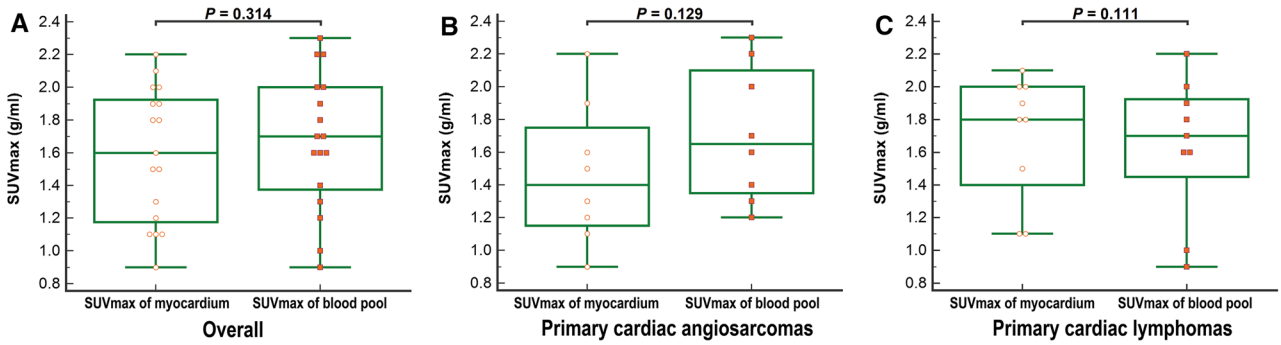

Figure 1. Mean comparison of ^{18}F-FDG uptake in the myocardium and blood pool. There were no differences in myocardial and blood pool uptake in the overall (**A**) or primary cardiac angiosarcoma group (**B**) or primary cardiac lymphoma group (**C**). *MTV* metabolic tumor volume; *TLR* tumor-to-liver ratio, *TLG* total lesion glycolysis.

Table 2. Quantitative evaluation of ^{18}F-FDG uptake agreement between the myocardium and cardiac blood pool

	SUVmax of myocardium (95% CI)	SUVmax of cardiac blood pool (95% CI)	*t*	*P* value
Overall	1.59 (1.38–1.80)	1.67 (1.46–1.88)	1.040	.314
Primary cardiac angiosarcomas	1.46 (1.10–1.82)	1.71 (1.37–2.06)	1.722	.129
Primary cardiac lymphomas	1.70 (1.41–1.99)	1.63 (1.30–1.97)	1.789	.111

Table 3. ^{18}F-FDG PET/CT and CECT imaging features of primary cardiac angiosarcomas and primary cardiac lymphomas

	All	Primary cardiac angiosarcomas	Primary cardiac lymphomas	*t* or *U*	*P* value
Number of patients	17	8	9		
Tumor morphology					.015*
Focal	7	6	1		
Diffuse	10	2	8		
Enhancement pattern					.002*
Homogeneous	7	0	7		
Heterogeneous	10	8	2		
Coronary artery floating sign	8	0	8		
SUVmax of Liver (95% CI)	2.87 (2.55–3.20)	2.62 (2.13–3.12)	3.09 (2.62–3.56)	1.576	.136
SUVmax (95% CI)	13.29 (9.75–16.84)	8.34 (5.57–11.10)	17.7 (12.90–22.50)	3.790	.002
SUVmean (95% CI)	6.98 (5.27–8.71)	4.42 (2.81–6.04)	9.26 (7.24–11.28)	4.273	.001
TLR (95% CI)	3.78 (2.72–7.04)	2.78 (2.29–4.40)	5.91 (3.76–8.04)	10.00	.011†
MTV (95% CI)	142.11 (32.14–244.61)	34.19 (8.30–133.059)	196.15 (143.39–270.72)	13.00	.027†
TLG (95% CI)	1260.39 (73.47–1763.75)	147.72 (32.57–623.09)	1764.06 (1497.26–2279.96)	4.000	.001†

*Fisher's Exact Test was used.
†Mann–Whitney *U* test was used.

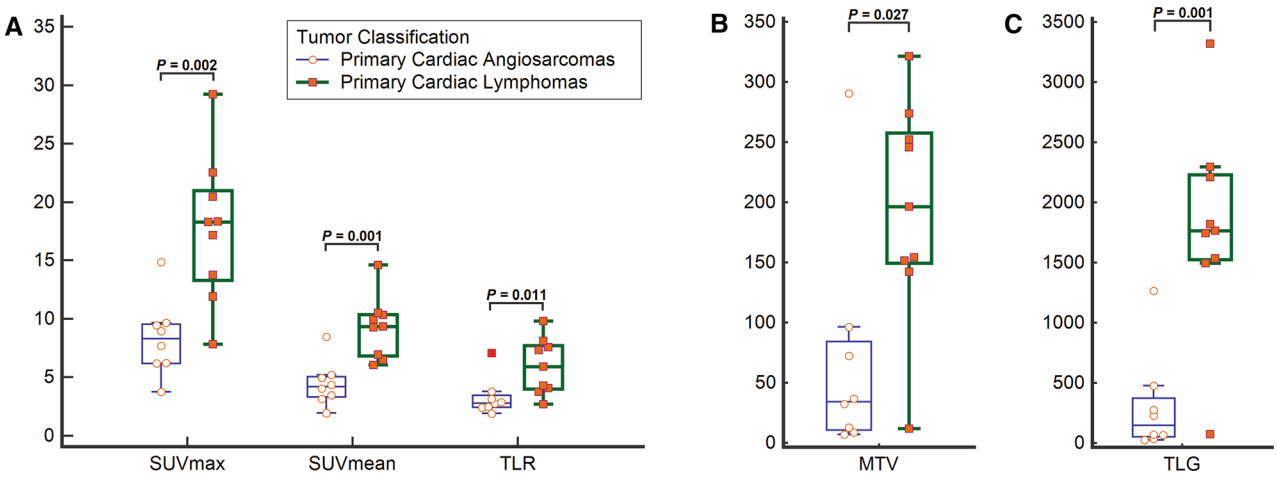

Figure 2. Comparison of ^{18}F-FDG uptake of tumors. There were significant differences in the mean of SUVmax (**A**) and SUVmean (**A**) and the median of TLR (A), MTV (**B**), and TLG (**C**) between primary cardiac angiosarcomas and primary cardiac lymphomas..

Table 4. ROC analysis for discriminating between primary cardiac angiosarcomas and primary cardiac lymphomas

	AUC	SE	*P* value	95% CI	Cutoff	Sensitivity (%)	Specificity (%)
CECT parameters							
Enhancement pattern	0.889	0.0735	< .001	0.644-0.987	-	77.78	100
Tumor morphology	0.819	0.0989	.001	0.561-0.960	-	88.89	75.00
PET/CT parameters							
SUVmean	0.958	0.047	< .001	0.738-1.000	> 5.17	100	87.5
TLG	0.944	0.059	< .001	0.718-0.999	> 1260.39	88.89	100
SUVmax	0.917	0.069	< .001	0.680-0.995	> 9.67	88.89	87.5
TLR	0.861	0.094	< .001	0.610-0.978	> 3.78	77.78	87.5
MTV	0.819	0.126	.011	0.561-0.960	> 96.3	88.89	87.5

AUC, area under the curve; *CECT*, contrast-enhanced CT; *CI*, confidence interval; *MTV*, metabolic tumor volume; *SE*, standard error; *TLG*, total lesion glycolysis; *TLR*, tumor-to-liver ratio

RESULTS

Population

Nine and eight patients with PCL and PCA were enrolled. All the patients had histopathological and immunohistochemical confirmation. The characteristics of the patients are shown in Table 1. A statistical difference in age between PCLs and PCAs (P = .025) was found. However, no statistical differences were found in gender (P = 1.000), blood glucose level (P = .099), and ^{18}F-FDG-injected dose (P = .286).

Of the nine cases with PCLs, five cases were confirmed by fine needle biopsies, two cases by cytological examinations of pleural and pericardial effusions, and the other two cases by partial resections. Of the eight cases with PCAs, two cases were confirmed by fine needle biopsies, one case by partial resection, and the other five cases by complete resections. Histologically, nine PCLs were classified as diffuse large B-cell lymphomas, the most common type of non-Hodgkin's lymphoma. None of the patients with PCLs had AIDS, as proven by a negative anti-HIV test.

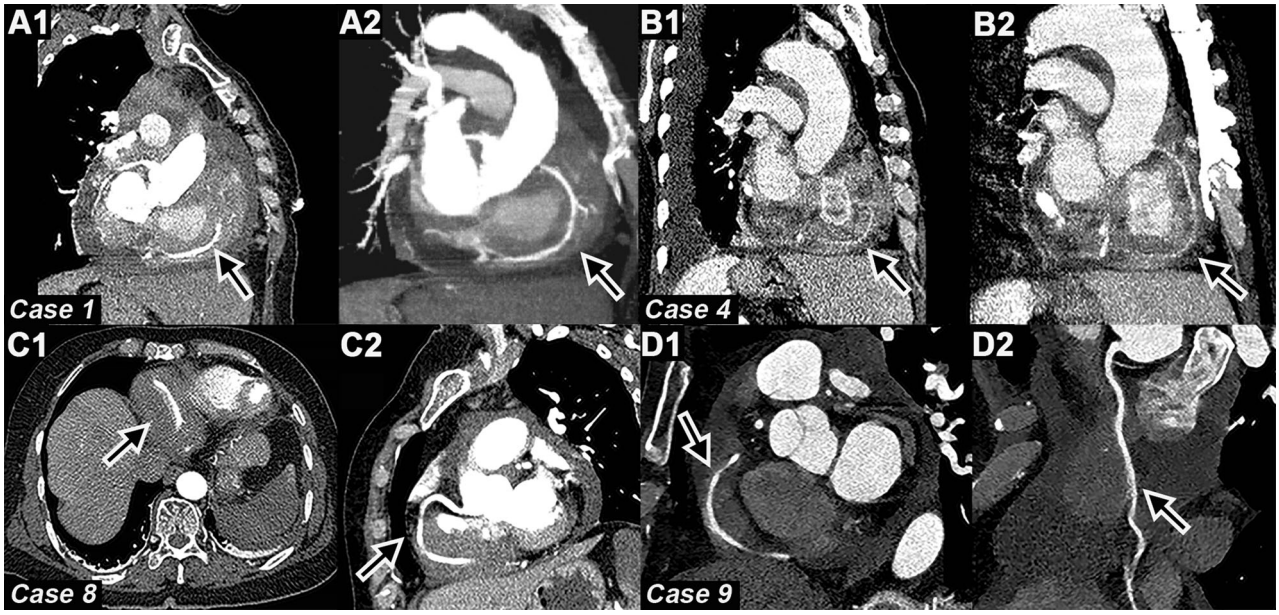

Figure 3. Right coronary vessel floating signs. **A**, **B**, **C**, and **D** represent four different patients with vessel floating signs. **A** and **B** show the right coronary artery (arrows) in two patients, respectively. Multiplanar reconstruction (1) and maximum intensity projection (2) show that the right coronary artery is encapsulated by the tumor without arterial invasion or compression (coronary vessel floating sign). The transverse (**C1**) and multiplanar reconstruction (**C2**) images showed that the tumor encased the right coronary artery (arrows) with no narrowing of the arterial lumen. Multiplanar reconstruction (**D1**) and curved multiplanar reformatted image (**D2**) showed that the tumor invaded the right coronary artery (arrows), and the wall of the latter was surrounded without stenosis..

Table 5. Diagnostic performance of various parameters

Feature	Sensitivity (%)	Specificity (%)	Positive predictive value (%)	Negative predictive value (%)	Accuracy (%)
Thoracic CECT alone	78	100	100	80	88
PET/CT alone*	89	75	80	86	82
Combined two modalities	89	88	89	88	88
PET/CT alone with cutoff $> 5.17^{\dagger}$	100	88	90	100	94
Combined two modalities with cutoff $> 5.17^{\dagger}$	100	100	100	100	100

*The diagnosis criteria do not contain cutoff values.
†SUVmean > 5.17

^{18}F-FDG PET/CT and CECT Images

From ^{18}F-FDG PET/CT images A quantitative evaluation of ^{18}F-FDG uptake agreement between the myocardium and blood pool was performed. In one case of PCLs (Case 5), the tumor filled the right ventricular cavity. It was poorly demarcated from the septum, so the

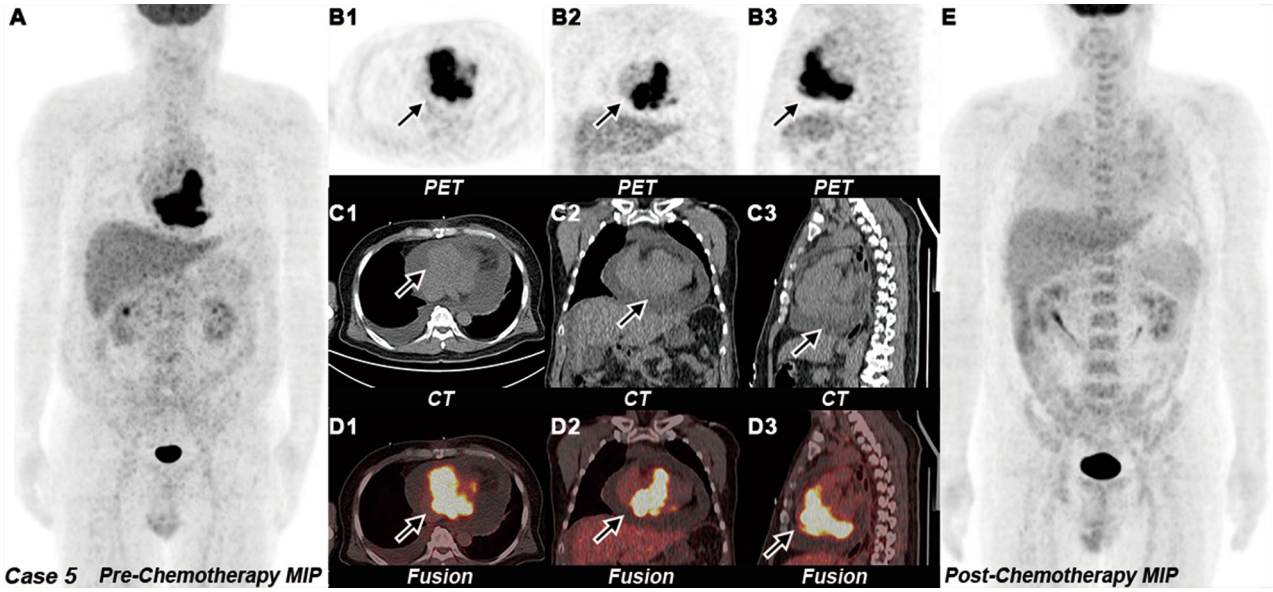

Figure 4. Primary cardiac lymphomas. MIP PET image before chemotherapy (**A**), ^{18}F-FDG PET (**B**), CT (**C**), fusion images (**D**), and MIP PET image after chemotherapy (**E**). Transverse (1), coronal (2), and sagittal images (3). **A** MIP image showing foci of uptake in the heart region before chemotherapy. **B**, **C**, and **D** showing a huge irregular mass with increased intense ^{18}F-FDG uptake (SUVmax: 18.3) in the atrioventricular groove (arrows). **E** MIP image showing an absence of clearly pathologic ^{18}F-FDG uptake in the heart region after chemotherapy, mild uptake in the bilateral lung region, and pulmonary inflammation confirmed by CT..

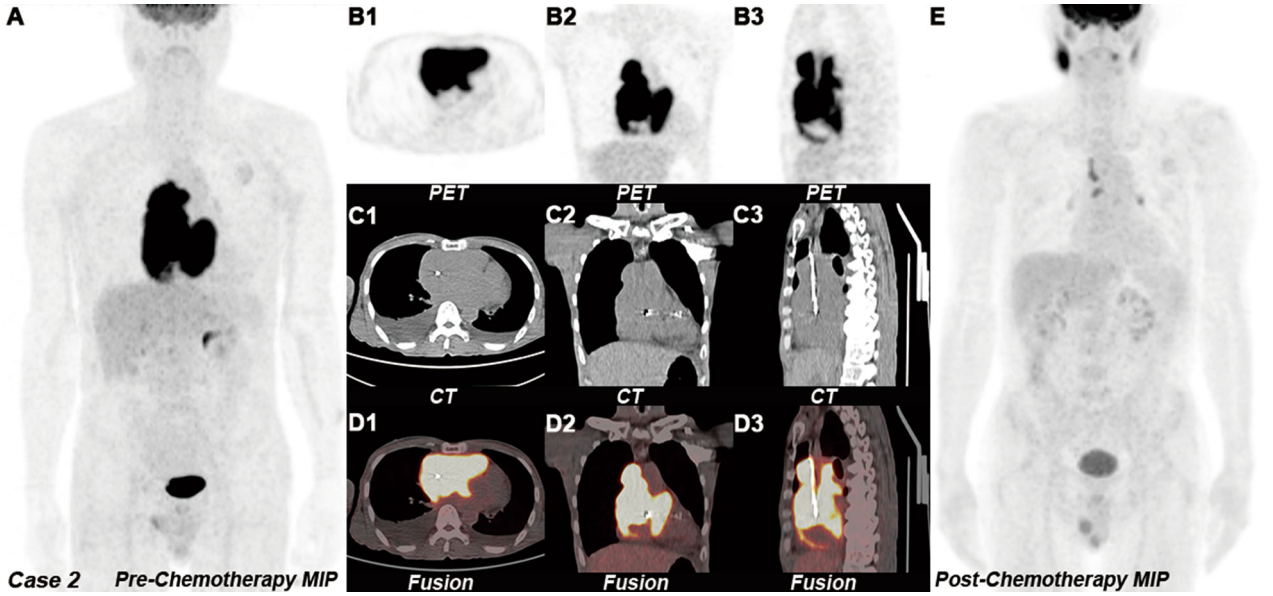

Figure 5. Primary cardiac lymphomas. MIP PET image before chemotherapy (**A**), ^{18}F-FDG PET (**B**), CT (**C**), fusion images (**D**), and MIP PET image after chemotherapy (**E**). Transverse (1), coronal (2), and sagittal images (3). **A** MIP image showing a huge lobulated mass with intense ^{18}F-FDG uptake in the heart region before chemotherapy and foci of ^{18}F-FDG uptake in the left upper lung region, which was confirmed to be a pacemaker. **B**, **C**, and **D** showing a huge irregular mass with increased intense ^{18}F-FDG uptake (SUVmax: 18.2) in the whole heart region. (**E**) MIP image showing the mediastinal and bilateral hilar lymph nodes with mild ^{18}F-FDG uptake and the bilateral masseter muscle with asymmetrical ^{18}F-FDG uptake after chemotherapy..

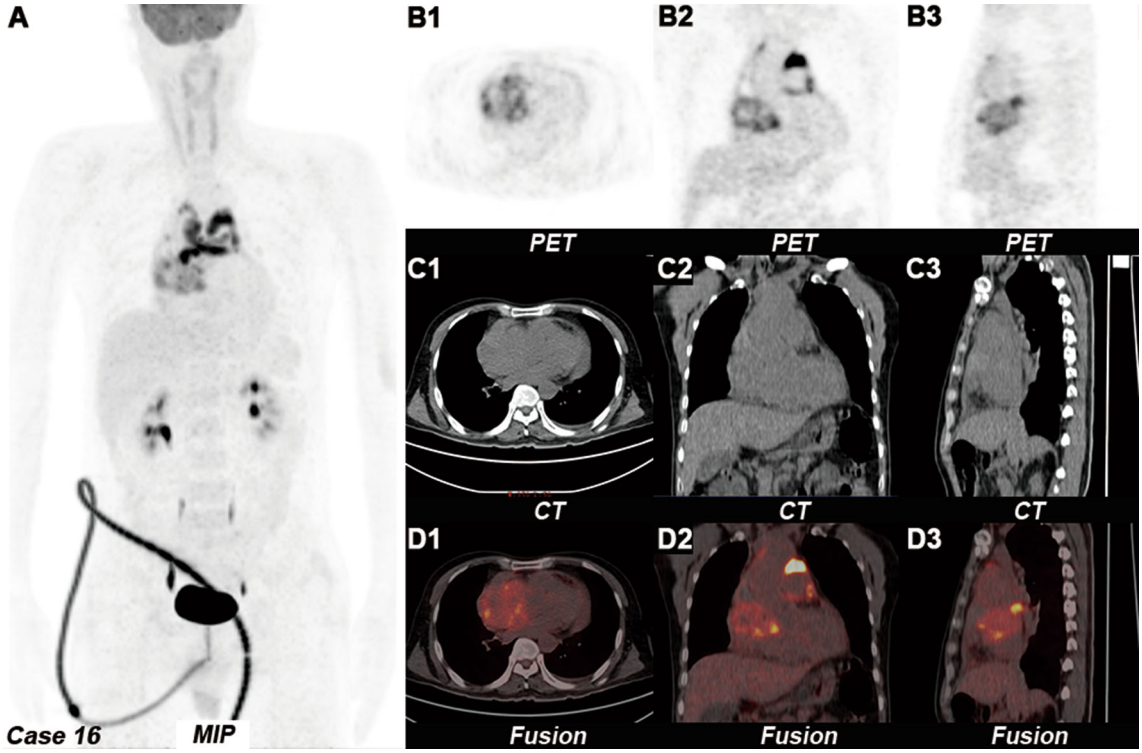

Figure 6. Primary cardiac angiosarcomas in the right atrium. MIP PET image (**A**), ^{18}F-FDG PET (**B**), CT (**C**), and fusion images (**D**). Transverse (1), coronal (2), and sagittal images (3). **A** MIP image showing multiple foci of uptake in the heart and mediastinal region. **B**, **C**, and **D** showing an irregular mass with increased uneven ^{18}F-FDG uptake (SUVmax: 14.8) in the right atrium..

SUVmax of the interventricular septum could not be measured. Therefore, in this case, the SUVmax of the LV free wall was measured. The interventricular septum was measured in the remaining cases (Supplementary Material 1). There was no significant difference in SUVmax between myocardial and blood pool uptake (Figure 1, Table 2). The mean of LVR was 0.97 (95% CI 0.87 to 1.07). There was no significant difference in the mean of LVR and the test value (Supplementary Material 2).

All the differences were statistically significant in SUVmax ($t = 3.790$, $P = .002$), SUVmean ($t = 4.273$, $P = .001$), MTV ($U = 13.00$, $P = .027$), TLR ($U = 10.00$, $P = .011$), and TLG ($U = 4.0$, $P = .001$) between PCLs and PCAs. The mean and median of the above subjects between PCLs and PCAs are detailed in Table 3 (Figure 2).

ROC analysis revealed that the highest AUC for SUVmean was 0.958 ($P < .001$, 95% CI 0.738-1.000), and the optimal cutoff value of SUVmean was 5.17, which could generate 100.0% sensitivity and 88% specificity (Table 4 and Supplementary Material 3).

From CECT Images There were significant differences in the enhancement pattern of tumors ($P = .002$) and the tumor morphology ($P = .015$). In nine cases of PCLs, seven cases showed homogeneous enhancement and the other two cases showed heterogeneous enhancement. All angiosarcomas showed heterogeneous enhancement. In nine cases of PCLs, eight cases showed diffuse lesions and the remaining one case showed focal lesions. In eight cases of angiosarcomas, six cases showed focal lesions and the remaining two cases showed diffuse lesions. The vessel floating sign was found in eight cases of PCLs (Figure 3). No floating sign was found in the remaining case because the lesion was located in the cardiac cavity. All lesions with angiosarcomas were located in the right atrium, and no sign of the vessel floating sign was found. A statistical difference in the tumor location between PCLs and PCAs ($P = .002$) was found. No statistical differences were found in pleural effusion ($P = .527$) or pericardial effusion ($P = .349$).

Diagnostic Performance of Two Modalities

PET/CT alone showed 89% sensitivity, 75% specificity, and 82% diagnostic accuracy. Thoracic CECT alone showed 78% sensitivity, 100% specificity, and 88% diagnostic accuracy. The combination of the two modalities showed 89% sensitivity, 88% specificity, and 88% diagnostic accuracy. Combined PET/CT and cutoff values (SUVmean $>$ 5.17) showed 100% sensitivity, 88% specificity, and 94% diagnostic accuracy. And combining both modalities and cutoff values (SUVmean $>$ 5.17) showed 100% sensitivity, 100% specificity, and 100% diagnostic accuracy (Table 5 and Supplementary Material 4). There were no significant differences between PET/CT alone or thoracic CECT alone and combined both modalities, with or without cutoff ($P >$ .05).

Outcome and Prognosis

Of the nine PCL cases, three patients achieved complete remission after chemotherapy with PET/CT (Figure 4 and 5 and Supplementary Material 5-6), two patients died, two patients showed partial remission after chemotherapy with CT, and the other two patients showed partial remission after chemotherapy with transthoracic echocardiography. Of the eight PCA cases (Figure 6, Supplementary Material 7), one patient underwent cardiac transplantation, two patients died, two patients developed distant metastases, and the other three patients were lost to follow-up.

DISCUSSION

This study is the first to describe the ^{18}F-FDG PET/CT and CECT imaging features of PCLs. This study provides the first comparative characterization of metabolic features between PCLs and PCAs, both of which arise in the right side of the heart. Combining of tumor enhancement pattern and morphology, as well as intensity- and volume-based PET parameters, helps distinguish PCLs from primary cardiac angiosarcomas and improves the accuracy of the diagnosis of PCLs (up to 100% in combination with cutoff values). Although the diagnostic accuracy tended to be higher in combined PET/CT and CECT than in a single modality, the differences were not statistically significant. The reason for this may be related to the small number of cases enrolled.

The current study found that the intensity-based PET parameters (SUVmax, SUVmean, and TLR) were significantly higher in PCLs than in PCAs. The mean value of SUVmax for PCLs was 17.7 (vs 8.34, $P < .05$), which was similar to the mean value of SUVmax (16.7) in the two cases with PCLs previously reported in our study. [15] It is also close to the mean value of SUVmax of two secondary cardiac lymphomas (15.2) reported by Rahbar et al. [19], six cases of secondary cardiac lymphoma (17.3) reported by Qin et al. [20] and seven cases of secondary cardiac lymphoma (19.4) reported by Meng et al.. [21] The mean value of SUVmax was significantly lower than that reported by Kikuchi et al. [22] in five cases of cardiac dominant lymphoma (25.9).

The current study found that the volume-based PET parameters (MTV and TLG) were significantly higher in PCLs than in PCAs ($P < .05$), implying that PCLs lesions are more extensively involved and diffuse. In contrast, PCAs lesions are more focal, consistent with the morphological characteristics of the tumor on CECT images.

The enhancement pattern of tumors was significantly different ($P = .02$) between PCLs and PCAs. In nine cases of PCLs, seven cases showed homogeneous enhancement and the other two cases showed heterogeneous enhancement. All angiosarcomas showed heterogeneous enhancement. It has been reported that the contrast enhancement of cardiac lymphoma may be homogeneous or heterogeneous with either modality. [23]

The tumor morphology was significantly different ($P = .015$) between PCLs and PCAs. Eight of the nine PCLs showed diffuse lesions, and the remaining one showed focal lesions. Six of eight angiosarcomas showed focal lesions and the remaining two showed diffuse lesions. Out of the nine PCLs, the tumors diffusely involved the heart wall and completely encased the coronary artery in eight cases, also called ''vessel floating sign.'' No floating sign was found in the remaining case because the lesion was in the cardiac cavity. In contrast, all lesions with angiosarcomas were in the right atrium, and no sign of the vessel floating sign was found. Since the PCL lesion mostly originates in the right atrium or atrioventricular sulcus, the lesion mostly encircles the right coronary artery, forming a right coronary artery floating sign, but there is no stenosis, which has been confirmed by coronary angiography.[24] The coronary artery floating sign is a specific characteristic of cardiac lymphoma.[14,22,25] Interestingly, one case of PCL had no vessel floating sign; the lesions were all located in the right atrial cavity, showing focal nodular protrusion into the cardiac cavity, without obvious infiltration, which was easily confused with angiosarcoma. Therefore, the diagnosis was very challenging.

It is worth noting that after dietary preparation, there was no significant increase in the myocardial glucose metabolism in all cases, which is helpful for the description of tumor lesions. However, for some patients who cannot follow a diet, such as those who are fasting,

the American Society of Nuclear Cardiology recommends low doses of IV heparin for suppression of myocyte glucose uptake.[26]

Unlike secondary cardiac lymphoma with superficial lymph node involvement, PCLs are difficult to diagnose by biopsy; therefore, it is important to use other non-invasive imaging methods. ^{18}F-FDG-PET/CT has proven to be an irreplaceable problem-solving tool and is preferred for routine staging and follow-up.

Limitations of Our Study

The limitations of this study are the small number of cases and the inherent defects of its retrospective nature. Second, there might be a selection bias. This limitation arises from our strict adherence to the narrow definition of PCLs.[4] According to this definition, cases were enrolled only if the lesion located in the heart was not accompanied by other organ or lymph node involvement, which potentially excluded cases with concurrent cardiac and other organs or lymph node involvement.

CONCLUSION

The average age of patients with PCL was significantly higher than that of patients with PCA. The intensity- and volume-based PET parameters of PCL were significantly higher than those of PCA. The enhancement pattern and tumor morphology were also different. The coronary artery floating sign is a specific characteristic of cardiac lymphoma. According to these characteristics, the two most common types of primary cardiac malignant tumors could be differentiated.

NEW KNOWLEDGE GAINED

Primary cardiac lymphomas (PCLs) are very rare. The most common location of the disease is similar to that of primary cardiac angiosarcomas (PCAs). Combined with the enhancement characteristics of the lesions and the intensity- and volume-based parameters of ^{18}F-FDG uptake, the two types of primary cardiac malignancies can be differentiated.

Author Contributions

(I) Conception and design: EL, JH, SW, and ZL. (II) Administrative support: SW and ZL. (III) Provision of study materials or patients: HD and ZC. (IV) Collection and assembly of data: EL, JH, CL, QX, and WX. (V) Data analysis and interpretation: EL, JH, and WX. (VI) Manuscript writing: All authors. (VII) Final approval of manuscript: All authors

Disclosure

All authors have completed the ICMJE uniform disclosure form. The authors have no conflicts of interest to declare.

Ethical Approval

The authors are accountable for all aspects of the work in ensuring that questions related to the accuracy or integrity of any part of the work are appropriately investigated and resolved. The study was conducted in accordance with the Declaration of Helsinki (as revised in 2013). The study was approved by the Research Ethics Committee of Guangdong Provincial People's Hospital (No. GDREC2019643H), and individual consent for this retrospective analysis was waived.

References

1. Roberts WC. Primary and secondary neoplasms of the heart. Am J Cardiol 1997;80:671-82.
2. Gowda RM, Khan IA. Clinical perspectives of primary cardiac lymphoma. Angiology 2003;54:599-604.
3. Nascimento AF, Winters GL, Pinkus GS. Primary cardiac lymphoma: clinical, histologic, immunophenotypic, and genotypic features of 5 cases of a rare disorder. Am J Surg Pathol 2007;31:1344-50.
4. Travis WD, Brambilla E, Burke AP, Marx A, Nicholson AG. WHO classification of tumors of the lung, pleura, thymus and heart, vol. 4. Lyon: IRAC; 2015. p. 340.
5. Burke A, Tavora F. The 2015 WHO classification of tumors of the heart and pericardium. J Thorac Oncol 2016;11:441-52.
6. Maleszewski JJ, Bois MC, Bois JP, Young PM, Stulak JM, Klarich KW. Neoplasia and the heart: Pathological review of effects with clinical and radiological correlation. J Am Coll Cardiol 2018;72:202-27.
7. Cichowska-Cwalińska N, Dutka M, Klapkowski A, Pęksa R, Maciej Zaucha J, Zaucha R. The role of radiotherapy in the management of primary cardiac lymphoma a case report and the literature review. Leuk Lymphoma 2019;60:812-6.
8. Bonou M, Kapelios CJ, Marinakos A, Adamopoulos S, Diamantopoulos P, Foukas PG, et al. Diagnosis and treatment complications of primary cardiac lymphoma in an immunocompetent 28-year old man: a case report. BMC Cancer 2019;19(1):191. https://doi.org/10.1186/s12885-019-5405-y.
9. Jeudy J, Burke AP, Frazier AA. Cardiac lymphoma. Radiol Clin N Am 2016;54:689-710.
10. Miguel CE, Bestetti RB. Primary cardiac lymphoma. Int J Cardiol 2011;149:358-63.
11. Xiao M, Lin J, Xiao T, Lin Y, Ye Y. The incidence and survival outcomes of patients with primary cardiac lymphoma: A SEER-based analysis. Hematol Oncol 2020;38:334-43.
12. Wang SC, Pan CW. Overcoming the diagnostic challenges in a high-risk invasive primary cardiac lymphoma. Eur Heart J Cardiovasc Imaging 2020;21:707.
13. Burke A, Jeudy J, Virmani R. Cardiac tumours: an update: Cardiac tumours. Heart 2008;94:117-23.
14. Colin GC, Symons R, Dymarkowski S, Gerber B, Bogaert J. Value of CMR to differentiate cardiac angiosarcoma from cardiac lymphoma. JACC Cardiovasc Imaging 2015;8:744-6.

15. Liu ET, Sun TT, Dong HJ, Wang SY, Chen ZR, Liu C, et al. Combined PET/CT with thoracic contrast-enhanced CT in assessment of primary cardiac tumors in adult patients. EJNMMI Res 2020;10:75. https://doi.org/10.1186/s13550-020-00661-x.
16. Boellaard R, Delgado-Bolton R, Oyen WJ, Giammarile F, Tatsch K, Eschner W, et al. FDG PET/CT: EANM procedure guidelines for tumour imaging: version 2.0. Eur J Nucl Med Mol Imaging 2015;42:328-54.
17. Sher A, Lacoeuille F, Fosse P, Vervueren L, Cahouet-Vannier A, Dabli D, et al. For avid glucose tumors, the SUV peak is the most reliable parameter for [18F]FDG-PET/CT quantification, regardless of acquisition time. EJNMMI Res 2016;6:21. https://doi.org/10.1186/s13550-016-0177-8.
18. Kang J-H, Youk JH, Kim J-A, Gweon HM, Eun NL, Ko KH, et al. Identification of preoperative magnetic resonance imaging features associated with positive resection margins in breast cancer: A retrospective study. Korean J Radiol 2018;19:897-904.
19. Rahbar K, Seifarth H, Schäfers M, Stegger L, Hoffmeier A, Tiemann K, et al. Differentiation of malignant and benign cardiac tumors using 18F-FDG PET/CT. J Nucl Med 2012;53:856-63.
20. Qin C, Shao F, Hu F, Song W, Song Y, Guo J, et al. 18F-FDG PET/CT in diagnostic and prognostic evaluation of patients with cardiac masses: A retrospective study. Eur J Nucl Med Mol Imaging 2020;47:1083-93.
21. Meng J, Zhao H, Liu Y, Chen D, Hacker M, Wei Y, et al. Assessment of cardiac tumors by 18F-FDG PET/CT imaging: Histological correlation and clinical outcomes. J Nucl Cardiol 2020. https://doi.org/10.1007/s12350-019-02022-1.
22. Kikuchi Y, Oyama-Manabe N, Manabe O, Naya M, Ito YM, Hatanaka KC, et al. Imaging characteristics of cardiac dominant diffuse large B-cell lymphoma demonstrated with MDCT and PET/CT. Eur J Nucl Med Mol Imaging 2013;40:1337-44.
23. Bligh MP, Borgaonkar JN, Burrell SC, MacDonald DA, Manos D. Spectrum of CT findings in thoracic extranodal non-hodgkin lymphoma. Radiographics 2017;37:439-61.
24. Chikata A, Sakagami S, Kanamori N, Kato C, Omi W, Saeki T, et al. Coronary vessel floating sign and vasospastic angina in a patient with cardiac lymphoma. Int J Cardiol 2014;176:e20-5. https://doi.org/10.1016/j.ijcard.2014.06.081.
25. Yoshihara S, Sugimoto Y, Matsunaga M, Suzuki S, Tanioka F. Coronary vessel floating sign in cardiac diffuse large B-cell lymphoma. Eur Heart J Cardiovasc Imaging 2020;21:233. https://doi.org/10.1093/ehjci/jez190.
26. Dilsizian V, Bacharach SL, Beanlands RS, Bergmann SR, Delbeke D, Dorbala S, et al. ASNC imaging guidelines/SNMMI procedure standard for positron emission tomography (PET) nuclear cardiology procedures. J Nucl Cardiol 2016;23:1187-226.